its external boundary, Fig. 2. The development of the copper microstructure under condition of the explosive bonding and its peculiarities were described in detail earlier [6, 7]. In particular, it has been shown that a fragmentation (grains subdivision to highly misoriented crystallites) inherent to metallic materials under severe plastic deformation is supplemented within the NNIZ by a deformation twinning. As it is seen in Fig. 2, near the external boundary of the NNIZ (Fig. 2a) the initial grains are only slightly distorted and only several traces of the deformation twins (near-twin boundaries according to Brandon criterion are marked by white) can be observed. In the middle of the NNIZ (Fig. 2b) both the development of fragmentation and intensive twining occur, but the initial grains still can be distinguished. Immediately near the bonding interface (Fig. 2c) one can observe rather uniform fragmented structure with an appearance of partial recrystallization. It is worth noted that the contribution of twinning in the microstructure formation near the bonding interface retains significant, however the deformation-induced deviation of their misorientations from the twin one exceed the bounds of Brandon interval.

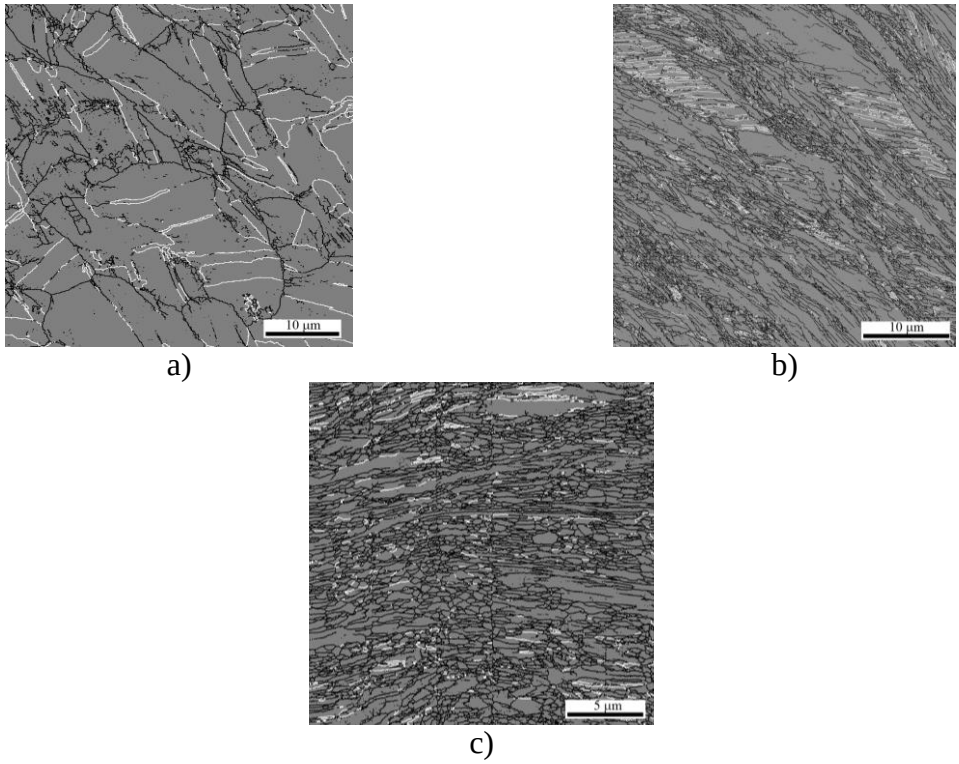

Fig. 2. Microstructure changes across the interfacial zone: near the external boundary of the NNIZ (a), in the middle of the NNIZ (b) and immediately near the bonding interface (c). The EBSD boundary maps display boundaries with $\theta > 2°$; near-twin boundaries according to Brandon criterion are drawn by white lines.

Three regions examined approximately correspond to the groups of points marked by dashed contours on the plot in Fig. 1 (denoted “a”, “b” and “c”). The average microhardness values obtained for these groups are 1856, 1742 and 1486 MPa. Then, in order to obtain data for the work-hardening plot, it is necessary to estimate local strains corresponding to these regions. This will be done in what follows from the analysis of misorientation distributions (Fig. 3) using the approach suggested recently [7].

According to the approach mentioned above, a misorientation distribution is represented as superposition of three components (partial distributions). The first one, which describes the low-angle peak of a distribution, is produced by deformation-induced boundaries (fragment or, in other terms, geometrically necessary boundaries [8]). The second component

corresponds to the twin boundaries (both annealing and deformation twins), which original twin misorientations were modified by a successive deformation. Remaining misorientations presumably associated with initial grain boundaries as well as the mostly misoriented fragments and the nuclei of recrystallization compose the third component, which can be described at first approximation using random misorientation distribution.

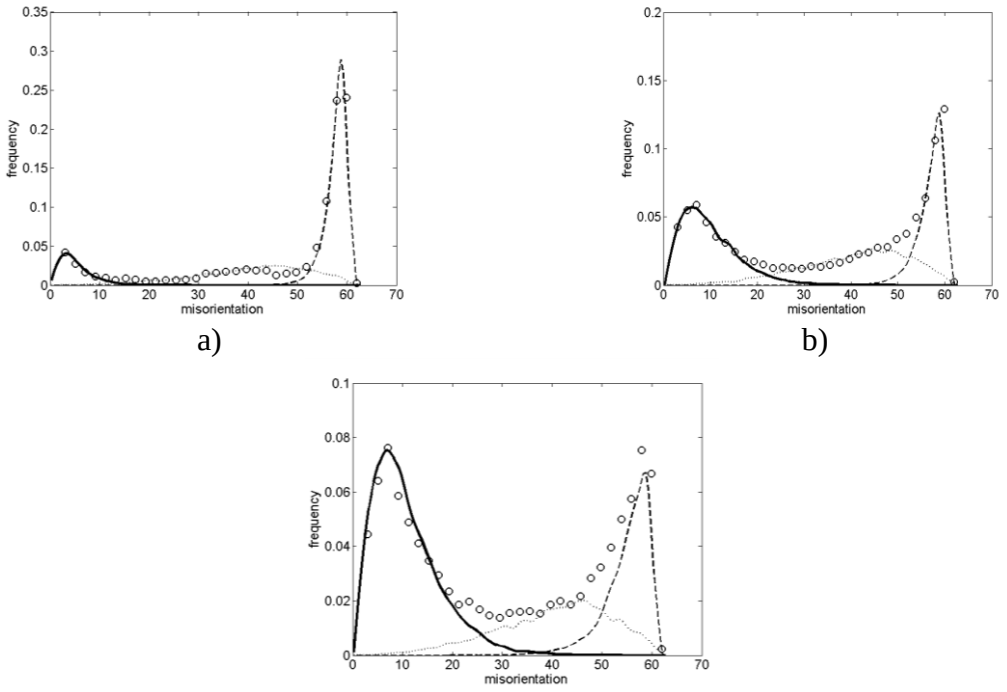

Fig. 3. Misorientation distributions obtained from the EBSD data for regions shown in Fig. 2(a, b, c), respectively, (round symbols), together with the calculated partial distributions for deformation-induced fragment boundaries (thick lines), deformation-modified twin boundaries (dashed line) and random boundaries (dotted line).

For the local strain estimation the first component can be employed. The misorientation distributions of the geometrically necessary boundaries $f(\theta)$ have been shown to collapse into a single distribution when scaled by the average misorientation θ_{av} [8]:

$$f(x) = \frac{a^a}{\Gamma(a)} x^{a-1} \exp(-ax), \qquad (1)$$

where $x = \theta/\theta_{av}$, a = 2.5. The dependence of the average misorientation on strain was shown to be $\theta_{av} = C\varepsilon^{2/3}$ with $C \approx 8°$ for geometrically necessary boundaries in the case of cold rolling of Al and Ni (strain rate $<10^1$ s^{-1}) [8,9]. Later on, similar θ_{av} dependence on ε was found for dynamically deformed Ni (strain rate ~ 10^3 s^{-1}) [10]. These literature data on average misorientations are presented in Fig. 4. It is seen that up to the strain of 1.5 the dependences almost coincide. The difference emerging at larger strains is resulted from the development of high-angle population of the deformation-induced boundaries, while the low-angle part of the distribution is described by Equation 1 as well.

Therefore, the increase of the strain rate by several orders of magnitude does not change considerably the parameters of the low-angle peak of the fragment misorientation distribution. With regard to this fact, one may try to use Equation 1 for approximation of low-angle peaks in the distributions shown in Fig. 3 and estimate a local strain for each region from the best fit

to the experimental data. The calculated distributions are shown together with the experimental ones in Fig. 3 (these distributions were determined based on EBSD data only for closed boundaries for better comparability with the results obtained earlier by TEM for geometrically necessary boundaries). The best fit of the low-angle peaks gives true local strains 0.5, 1.4 and 1.6 for regions a, b and c, respectively.

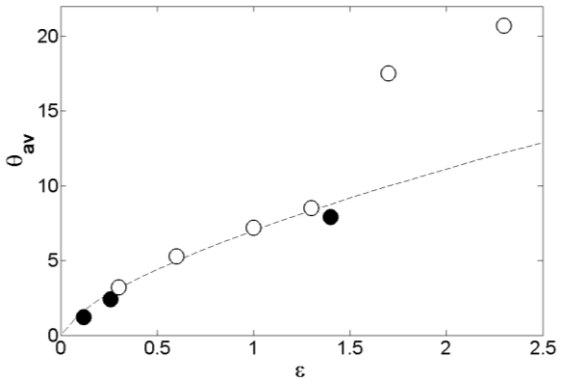

Fig. 4. Average misorientation angle as function of strain for Ni deformed by dynamic plastic deformation (full round symbols) [10] and by cold rolling (open round symbols) [9].

The resulting dependence of microhardness versus strain in the near-interface zone of the explosive joint is presented in Fig. 5. For comparison, approximation of microhardness measurements in copper deformed by torsion up to various strains [11] is shown by the dashed line. It is seen that for small strains the microhardness agrees well with literature data. At the same time, after $\varepsilon \geq 0.5$ the work-hardening observed in the NNIZ turns out to be considerably higher. The following causes can lead to this behavior. The first (and supposedly the most important) one is associated with deformation twinning, which takes place in copper only under extremely high strain rates, such as in the case of explosive bonding (~10^6 s^{-1}). A submicron fragmented structure is formed both under low and high strain rates leading to strengthening of a deformed material, which is well described by Hall-Petch type relationship: $\Delta\sigma = kD^{-1/2}$. However, for low-angle boundaries with misorientation angles $\theta < 15°$ the slope $k \sim \sqrt{\theta}$ smaller than the slope for high-angle boundaries, which does not depends on θ [12, 13]. The deformation twinning results in increasing fraction of high-angle boundaries within the fragmented structure [6]. Hence, the strengthening will be enhanced in this case. The second cause of increased strengthening may be associated with a probable decreasing of the fragment size D with increasing strain rate [10], however, additional study is needed concerning this issue.

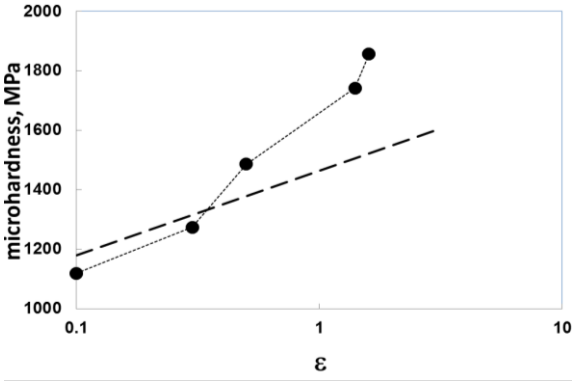

Fig. 5. Variation of microhardness as a function of local plastic strain near the bonding interface of the copper/copper joint.

4. Conclusions

Work-hardening behavior of copper was studied using a specimen obtained by explosive bonding on the base of the microhardness measurements and the microstructure examination across the near-interface zone of strongly inhomogeneous deformation. The local strains in different regions within the NNIZ have been evaluated based on the analysis of the distribution of misorientations at deformation-induced boundaries. Dynamic deformation twinning was shown to give significant contribution to the fragmented microstructure formation. This twinning causes accelerated work-hardening as compared to the copper deformed with a conventional strain rate.

Acknowledgments.

This work was supported by the Russian Science Foundation, project No. 15-13-20030.

References

[1] V.I. Lysak, S.V. Kuzmin, *Explosive Welding* (Mashinostroyeniye, Moscow, 2005). (In Russian).

[2] J. Song, A. Kostka, M. Veehmayer, D. Raabe // *Materials Science and Engineering A* **528** (2011) 2641.

[3] V.V. Rybin, E.A. Ushanova, S.V. Kuzmin, V.I. Lysak // *Technical Physics Letters* **37** (2011) 1100.

[4] V.V. Rybin, E.A. Ushanova, N.Yu. Zolotorevsky // *Technical Physics* **58** (2013) 1304.

[5] H. Paul, L. Lityńska-Dobrzyńska, M. Prażmowski // *Metallurgical and Materials Transactions A* **44A** (2013) 3836.

[6] V.V. Rybin, N.Yu. Zolotorevsky, E.A. Ushanova // *Technical Physics* **59** (2014) 1819.

[7] V.V. Rybin, N.Yu. Zolotorevsky, E.A. Ushanova // *Physics of Metals and Metallography* **116** (2015) 730.

[8] D.A. Hughes, Q. Liu, D.C. Chrzan, N. Hansen // *Acta Materialia* **45** (1997) 105.

[9] D.A. Hughes, N. Hansen // *Acta Materialia* **48** (2000) 298.

[10] Z.P. Luo, H.W. Zhang, N. Hansen, K. Lu // *Acta Materialia* **60** (2012) 1322.

[11] A. Dubravina, M.J. Zehetbauer, E. Schafler, I.V. Alexandrov // *Materials Science and Engineering A* **387–389** (2004) 817.

[12] N. Hansen, X. Huang, G. Winther // *Materials Science and Engineering A* **494** (2008) 61.

[13] A. Iza-Mendia, I. Gutierrez // *Materials Science and Engineering A* **561** (2013) 40.